Journal of the Civil Engineering Forum, September 2023, 9(3):277-286
DOI 10.22146/jcef.6749
Available Online at https://jurnal.ugm.ac.id/v3/jcef/issue/archive

Seismic Performance Evaluation of Wharf Based on ASCE 61-14

Kukuh Adhi Kafie[1,*], Andreas Triwiyono[1], Iman Satyarno[1], Hsuan-Teh Hu[2]
[1]Department of Civil and Environmental Engineering, Universitas Gadjah Mada, Yogyakarta, INDONESIA
Jalan Grafika No 2 Yogyakarta
[2]Department of Civil Engineering, National Cheng Kung University, TAIWAN
*Corresponding author: adhikafie@mail.ugm.ac.id

SUBMITTED 18 January 2023 **REVISED** 31 March 2023 **ACCEPTED** 15 May 2023

ABSTRACT The adequacy of the structural performance of a wharf in withstanding seismic loads is of paramount importance. Therefore, this research aims to conduct an accurate pushover analysis on the adequacy of a wharf located in North Sulawesi, Indonesia. The study provides a comprehensive overview of the seismic performance of the wharf by examining displacement and strain parameters of its plastic hinge components under various loading conditions. To simulate accidental torsion, the wharf structure was analyzed by introducing variations in the eccentricity offset of the lateral pushover load of -5%, 0%, and 5% from the center of mass. The analysis of the torsion behavior involved a comprehensive examination of four control points located at each corner of the wharf plan. Additionally, the investigation took into account, the crucial aspect of soil-structure interaction by considering the equivalent fixity depth of the pile, which was used to evaluate the fixity length of the structure. In order to determine the target displacement of the wharf, analysis was performed in accordance with the established methodologies outlined in FEMA-356. It is also important to note that the seismic performance of the wharf was evaluated based on acceptance criteria in the form of strain limits imposed on various components, including concrete elements, reinforcing steel, and steel pipes, as prescribed by ASCE 61-14. In this study, a total of 30 models were examined, and the obtained results showed that the structure exhibited controlled and repairable damage even when subjected to a 475-year earthquake return period (CLE: Contingency Level Earthquake). Following this, the analysis of variations in displacement control point served to determine the inherent torsion exhibited by the structure, and the introduction of different lateral load eccentricity offsets and variations in pushover loading direction were found to contribute to the increased displacement and strain in the plastic hinge components.

KEYWORDS Wharf; Pushover Analysis; Accidental Torsion; Plastic Hinge; Target Displacement.

1 INTRODUCTION

A wharf plays a crucial role in the transportation of coal, which is used to generate heat for steam turbines. Since they serve as the primary entry point for coal transported by barges from mines, it is essential to evaluate their post-designed structural integrity. These evaluations allow for accurate prediction of seismic performance, particularly during earthquakes. In this regard, a wharf must possess excellent structural performance, particularly in its ability to withstand lateral seismic loads.

The ASCE 61-14 Seismic Design on Piers and Wharves (ASCE, 2014) code specifies the minimum seismic design standards for non-public-access wharf. These standards have been in use since the implementation of SNI 1726:2019 (Nasional, 2019), which was also incorporated in ASCE 7 (2010, 2016, 2022) for non-building structures, such as piers and wharves, that are open to the public. Accordingly, ASCE 61-14, structures classified as high-piled must meet the requirements for controlled and repairable damage (CRD) performance level when subjected to a design earthquake with a return period of 475 years. At the controlled and repairable damage performance level, significant spalling is allowed until the reinforcement at the junction of the pile and slab is exposed.

Several studies have been conducted to evaluate the seismic performance of a wharf based on the acceptance criteria outlined in ASCE 61-14. Such studies have been conducted by Hanifah et al.

(2017); Bergman et al. (2016); Palma-ochoa and Vasquez (2019); Su et al. (2021), while Venkatalakshmi et al. (2017) and Zacchei et al. (2019) used the acceptance criteria of Applied Technology Council, ATC-40 (1996) as a reference. Bruin et al. (2016); Goel and Goel (2017); Goel (2018), and Sandoval et al. (2019) have also reported that the substitute structure method for determining the target displacement based on ASCE 61-14 produces overestimated and underestimated results on structures with short and longer periods respectively. However, none of these studies have specifically examined the seismic performance of a wharf in relation to accidental torsion.

The aim of this study is to evaluate the seismic performance of a wharf building using pushover analysis following ASCE 61-14 acceptance criteria. The analysis considered a 475-year return period earthquake scenario. Furthermore, to simulate accidental torsion, the wharf structure was analyzed with variations in eccentricity offset of the lateral pushover load, ranging from -5%, to 5% from the center of mass. This study is primarily focused on assessing displacement and strain behavior at all control points and loading directions.

By analyzing seismic performance of wharf structures, authorities are being provided with relevant insights to help them determine their next assessment step. Admittedly, owners and engineers will benefit from a better understanding of the seismic performance of these structures, particularly those investigated in this study. The findings can also be applied in earthquake-prone regions to conduct their seismic performance evaluations.

2 METHODS

This study comprised two stages of pushover analysis. The first stage was focused on determining the target displacement at the central mass point of the six created models. Moreover, the second stage was conducted to determine the strain experienced by the plastic hinge component when the monitored displacement was equal to the value of the target displacement obtained in the first stage. It is also important to note that in this study, the displacement and strain behavior at four control points positioned at the seaside and landside corners were investigated. In total, 30 displacement and strain parameter data were discovered.

2.1 Structural Data

This study used the pre-existing structural data of the wharf located in North Sulawesi, Indonesia, measuring 67×7.5 meters. The wharf was constructed using a total of 147 steel pipe piles, each of which has a diameter of 1000 mm, with a yield strength of 240 MPa. Among these, 119 of the piles used had a thickness of 16 mm, while 28 possessed a thickness of 19 mm. These piles were positioned at the landside corner of the wharf plan, as shown by the yellow circles in Figure 1. For the deck (slab) and beam sections, a concrete material with a strength of 30 MPa was used, accompanied by reinforcing steel with a yield strength of 400 MPa. Accordingly, the wharf structure was supported by steel pipe piles and beams with dimensions of 40×70 cm. The slab section was made with a uniform thickness of 35 cm, and a pile cap structure measuring 200×200×100 cm was constructed at the top of each pile, as shown in Figure 2. To establish a composite action between the steel pipe joint and the pile cap, a 3 m depth pile head treatment (PHT) was implemented at the top of each pile.

The earthquake design response spectrum parameters at the wharf site were evaluated in accordance with the SNI 1726:2019 (Nasional, 2019) standard. Seismic design considered the site class category of soft soil (SE), and the corresponding response spectrum can be seen in Figure 3.

2.2 Structural Modelling

The wharf structure, as shown in Figure 4, was modeled in 3D using the SAP2000 software. The modeling process focused solely on the structural components, namely the wharf platform (slab), pile cap, beam, and pile. In accordance with seismic load provisions outlined in ASCE 61-14, POLB (2012, 2015, 2021), the applied loads for analysis included the self-weight of the structure, permanently installed equipment and 10% of the uniform live load design. Furthermore, to incorporate nonlinear behavior, the plastic hinge were defined in accordance with the existing section data using the fiber P-M2-M3 type, both at the top and bottom of the piles. The decks and beams were modeled linearly, adhering to the criteria outlined in ASCE 61-14 passage 3.8, where it was

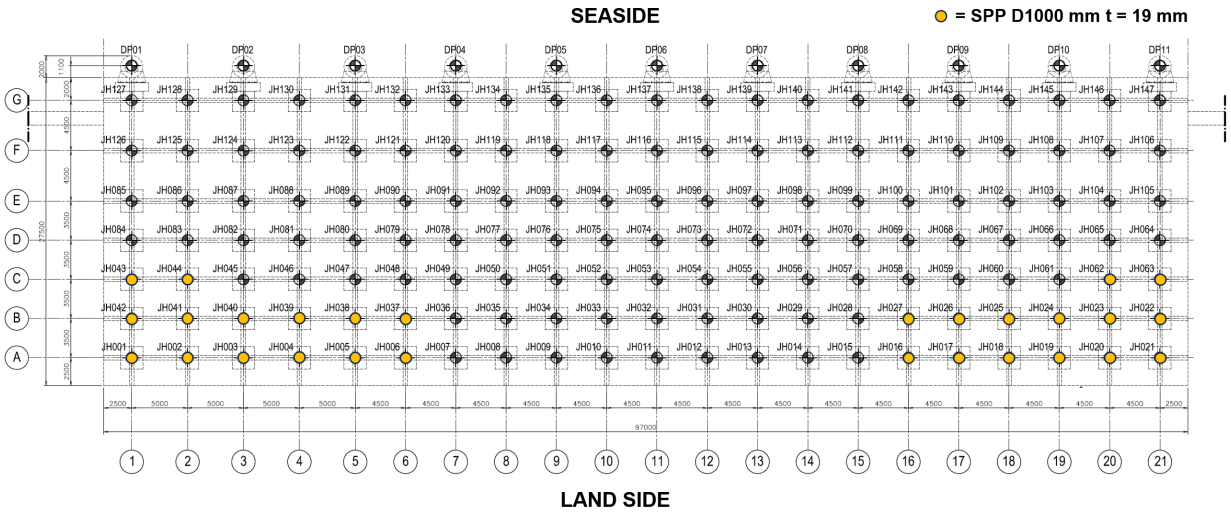

Figure 1 Plan view of the wharf structure

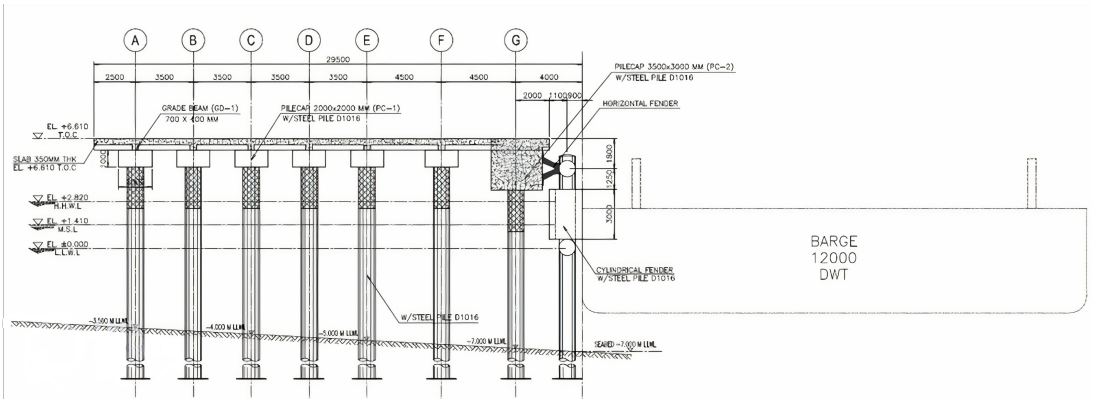

Figure 2 Typical lateral cross-section of the wharf structure

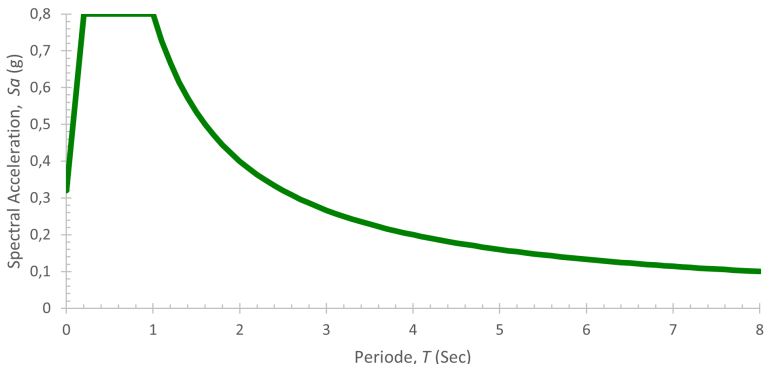

Figure 3 Spectrum response design using SNI 1726:2019 (Nasional, 2019)

stated that the deck (including beams) should be designed as a capacity-protected element. For pushover analysis, a nonlinear static load case was defined in the SAP2000 software, incorporating lateral load input in the form of a quake-type load pattern. The load pattern was calculated based on the static equivalent earthquake load according to the specifications of SNI 1726:2019 (Nasional, 2019). Throughout the study, the eccentricity ratio and seismic load direction were varied while defining the load pattern. Lastly, analysis of pile foundation fixity length was conducted by first identifying the location of the study object and then adjusting the corresponding soil data. The cal-

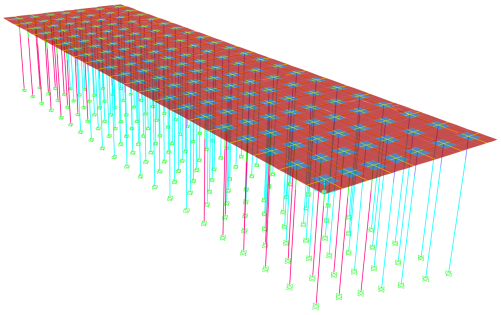

Figure 4 3D Structural model

culation of the fixity length was performed in accordance with the procedures and equations outlined in FEMA (2011). Alternatively, the pile fixity length can also be calculated using the equations provided in The Overseas Coastal Area Development Institute of Japan, OCDI (2009).
This study primarily focuses on investigating the impact of accidental torsion, which may arise from various factors, such as the asymmetric distribution of lateral ground motions across the building plan, asymmetric stiffness contributed by the gravity system of the structure, or nonstructural elements that were not considered in the design, irregular distribution of live loads, or changes in the center of rigidity due to nonlinear behavior. To address all potential sources of accidental torsion, ASCE 7 (2010, 2016, 2022) stipulated that buildings with rigid diaphragms should consider the design moment resulting from accidental torsion, in addition to any inherent torsion that may be present. The design moment of accidental torsion is calculated as torsion due to the application of seismic loads with an offset of 5% on the building dimension to the center of mass, perpendicular to the applied lateral load. This provision led to an increase in the base shear design of frame structures and lateral force-resisting walls.

It is crucial to consider the provisions for accounting the effect of torsion, as regulated by SNI 1726:2019 (Nasional, 2019). This process involves taking into account, the inherent torsion resulting from the difference between the center of mass and that of rigidity at each level during analysis. Accidental torsion must also be taken into consideration, especially for structures with Types 1a and 1b horizontal irregularities. This torsion involved assuming a displacement of the center of mass from its actual location by a distance equal to 5% of the diaphragm dimension of the structure parallel to the mass drift direction. Following this, the determination of the required eccentricity of 5% from the center of mass did not need to be performed simultaneously in both orthogonal directions. It is also important to note that the variations in eccentricity ratio values of -5%, 0%, and 5% were applied when defining the load pattern in the SAP2000 software.

The pushover analysis was conducted in two stages. The first stage aimed to determine the target displacement value at the monitored displacement point. Meanwhile, in the second stage, the previously obtained strain, occurring in the plastic hinge at the target displacement value was evaluated.

2.3 The Target Displacement and Strain Limit

A comprehensive analysis was conducted to assess the displacement of the wharf structure. This analysis was carried out in accordance with displacement–base shear force curve obtained from the pushover analysis. To determine the target displacement, the FEMA (2000) method, was employed. This involved creating a bilinear idealization curve based on the relationship between displacement and base shear force at the monitored displacement point. As shown in Figure 5, the bilinear curve was generated iteratively and the areas under it and the original curve were approximately equal. Furthermore, to establish the effective lateral stiffness, K_e, a line was drawn to intersect the actual curve at a point corresponding to 60% of the effective yield strength, 0.6 V_y. The slope of the post-yield bilinear curve, denoted as α, was determined by drawing a line from the point of the effective yield strength, V_y, to intersect the actual curve at the calculated target displacement point. It is important to note that the effective yield strength, V_y, should never exceed the base shear force value at any point along the actual curve.

To evaluate the structural integrity of the wharf under the designated load, a strain limit analysis was conducted. This analysis specifically focused on examining the strain experienced by the plastic hinge components of the structure during an earthquake scenario with a 500-year return period. The observed strain values were then compared to the predefined acceptance criteria for controlled

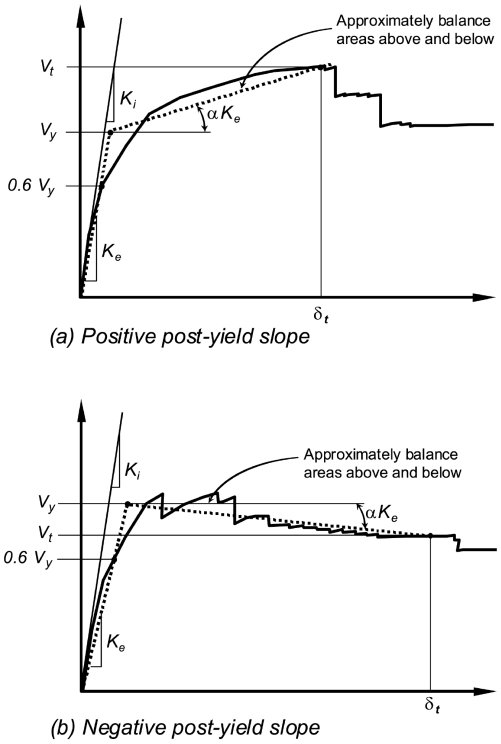

Figure 5 Idealized forced–displacement curves (FEMA-356)

and repairable damage, as outlined in ASCE 61-14 (Table 1). By comparing the observed strain values with the acceptance criteria, the performance level of the wharf structure could be determined. The primary emphasis of the strain limit analysis in this study was to characterize the behavior of local member, particularly the hinges, as they significantly influence the seismic performance of the structure. However, it is important to note that the overall performance of the wharf structure, typically represented by the drift ratio parameter, was not considered in this paper. This decision adheres to the guidelines specified in ASCE 61-14 (passage 5.4.1.4) and SNI 1726:2019 (passage 10.3.5), where it was stated that drift ratio does not need to be taken into account for the main platform structure of wharves and nonbuildings, but should be considered for ancillary components.

3 RESULTS

3.1 Fixity Length Analysis Result

The results of the soil investigation showed that each soil layer possessed a medium to dense density. According to (Terzaghi, 1955), the coefficient of modulus of variation, denoted as n_h, was assumed to be 7.5 MN m^{-3} or 7500 kN m^{-3}. Furthermore, the material used for the pile was steel pipes with a modulus of elasticity, E, of 200000 MPa, a moment of inertia, I, of 0.0063 m^4, and its foundation fixity length, d, was calculated using the following formulas.

$$d = 1.8\left(\frac{EI}{n_h}\right)^{\frac{1}{5}} = 1.8\left(\frac{200000\times1000\times0.0063}{7500}\right)^{\frac{1}{5}} = 5\text{m}$$

Table 1. Strain limit on hinge component of steel pipe pile (ASCE 61-14)

Performance Level	Component	Hinge Location		
		Top of pile	In-ground	Deep in the ground (>10D_p)
Controlled and Repairable Damage	Steel Pipe		$\varepsilon_s \leq 0.025$	$\varepsilon_s \leq 0.035$
	Concrete Reinforcing Steel	$\varepsilon_c \leq 0.025$ $\varepsilon_s \leq 0.6\,\varepsilon_{smd} \leq 0.060$		

* if the steel pipe pile is infilled with concrete, a value of 0.035 may be used.
ε_{smd} is the strain at peak stress of dowel reinforcement

3.2 The Target Displacement Analysis Result

The target displacement analysis was performed at the center of mass location (Point X in Figure 6) for the six different variations of the model. Accordingly, the displacement values at the control points (Points A, B, C, and D), which were obtained from the previous step (second running results), were used to examine the displacement behavior of the structure under various variations. This resulted in a total of 30 displacement values, as shown in Table 2, Table 3, and Figure 7. Among the model variations subjected to pushover loading with a 500-year return period earthquake scenario, the POX$_{-5\%}$-500$_{yr}$-B model exhibited the largest displacement value, which was 0.18806, along the X-axis. On the other hand, the POY$_{5\%}$-500$_{yr}$-B model recorded the highest displacement value of 0.16404 m for pushover loading in the Y-axis direction. The analysis results were presented for each group of model variations, taking into account, the displacement control point, eccentricity offset, and pushover lateral load direction.

The analysis of displacement control point variations showed that the structure exhibited inher-

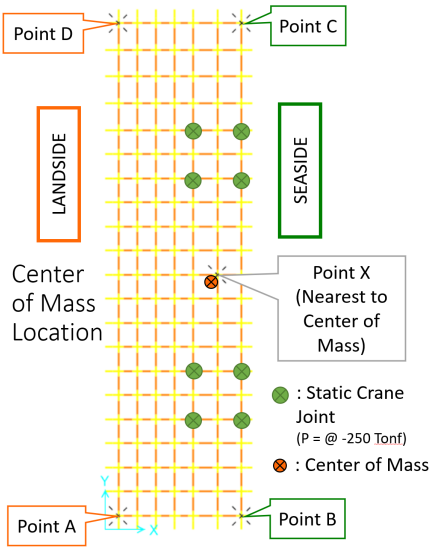

Figure 6 Location of the center of mass and control joint

ent torsion towards the east zone (Points A and B) when subjected to pushover loading along the X-axis direction, and towards the seaside zone (Points B and C) when loaded along the Y-axis direction. When examining the displacement in the X-axis loading direction with a 0% eccentricity offset, the dominant displacement value was observed in the eastern zone, which became even more pronounced with a -5% eccentricity offset (same direction of rotation as the inherent torsion). Conversely, a 5% eccentricity offset in the X-axis loading direction resulted in a displacement opposite to the inherent torsion direction. In the Y-axis loading direction, however, a 5% eccentricity offset was insufficient to counteract the impact of the inherent torsion of the structure. This resulted in displacement dominating in the same direction as the inherent torsion.

Regarding the analysis of eccentricity offset variation, it was found that the addition of a lateral load eccentricity offset of ±5% increased the displacement, particularly along the weak axis (X-axis). The magnitude of the additional moment was directly proportional to the length of the moment arm, which was influenced by the eccentricity and depth of the field. Along the weak axis (X-axis), the depth of the field extended longitudinally towards the wharf, while in the direction of the strong axis (Y-axis), it extended transversely.

Following this, the pushover analysis conducted in the direction of the strong axis (Y-axis) yielded displacements that closely corresponded to the expected behavior, even more significantly than the pushover analysis along the weak axis (X-axis). Based on these findings, it is essential to include pushover analysis in both orthogonal directions in order to gain a more comprehensive understanding of all potential failure mechanisms.

3.3 Strain Limit Analysis Result

The strain limit analysis involved re-running pushover analysis by adjusting the load to match the monitored displacement magnitude value in pushover load case according to the target displacement value at point X. Figure 8 shows the fiber strain report obtained from the SAP2000 software for one of the models.

In order to assess seismic performance of the wharf structure, the strain values in the plastic hinge components at the bottom of the pile (in-ground) were compared to the acceptance criteria outlined in ASCE 61-14. This comparison was conducted at multiple points, including location Points X, A, B, C, and D, during the final step of the second running phase (Figure 9 and Figure 10). From analysis, it was found that the wharf structure still satisfied the structural performance requirements according to ASCE 61-14, and all models exhibited controlled and repairable damage performance. According to ASCE 61-14, controlled and repairable damage is performance level typically associated with structures designed to withstand earthquakes with a return period of 475-500 years.

The results of the strain analysis based on the variation of displacement control points showed that the land side (points A and D) experienced the highest strain on all the plastic hinge components. This indicated that the maximum strain occurred at the stiffest side of the building, corresponding to the shorter pile length of the model.

The investigation of strain variation due to eccentricity offset variation showed that adding a ±5% ratio increased the strain on the plastic hinge components under pushover loading along the weak axis (X-axis) at all positions. However, the addition of lateral load eccentricity offset did not significantly increase the strain on pushover loading in the strong axis (Y-axis) direction. The strain analysis of the plastic hinge component in the di-

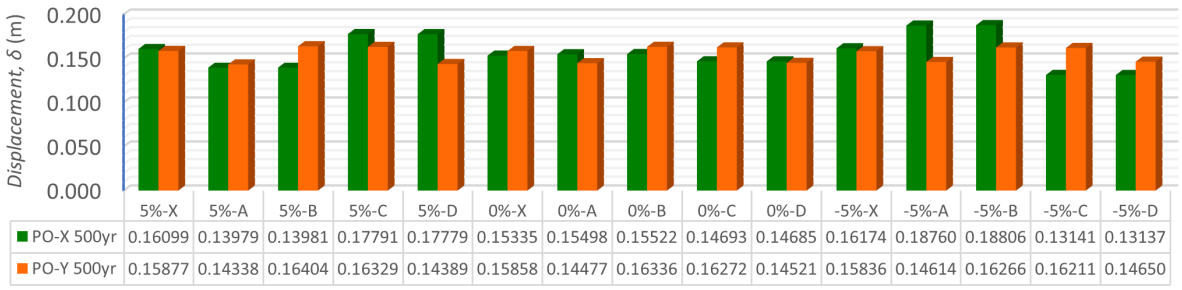

	5%-X	5%-A	5%-B	5%-C	5%-D	0%-X	0%-A	0%-B	0%-C	0%-D	-5%-X	-5%-A	-5%-B	-5%-C	-5%-D
PO-X 500yr	0.16099	0.13979	0.13981	0.17791	0.17779	0.15335	0.15498	0.15522	0.14693	0.14685	0.16174	0.18760	0.18806	0.13141	0.13137
PO-Y 500yr	0.15877	0.14338	0.16404	0.16329	0.14389	0.15858	0.14477	0.16336	0.16272	0.14521	0.15836	0.14614	0.16266	0.16211	0.14650

Figure 7 Displacement in all nodes of all variations

Table 2. Displacement, strain, and performance level for pushover in X-axis under the 500-year return period earthquake scenario

Node	Displacement (m)	Steel Pipe		Concrete	Reinf. Steel	Performance Level
		Strain (Tension)	Strain (Compression)	Strain (Compression)	Strain (Tension)	
Performance Point PO-X Eccentricity = +0.05						
X	0.16099	0.001442	-0.001642	-0.000737	0.000977	<CRD
A	0.13979	0.001843	-0.001439	-0.000494	0.000688	<CRD
B	0.13981	0.000864	-0.001213	-0.000511	0.000530	<CRD
C	0.17791	0.001154	-0.001679	-0.000629	0.000686	<CRD
D	0.17779	0.002776	-0.002056	-0.000580	0.000799	<CRD
Performance Point PO-X Eccentricity = 0.00						
X	0.15335	0.001342	-0.001515	-0.000707	0.000931	<CRD
A	0.15498	0.002147	-0.001710	-0.000532	0.000735	<CRD
B	0.15522	0.000974	-0.001356	-0.000561	0.000588	<CRD
C	0.14693	0.00093	-0.001263	-0.000531	0.000566	<CRD
D	0.14685	0.001984	-0.001569	-0.000513	0.000709	<CRD
Performance Point PO-X Eccentricity = -0.05						
X	0.16174	0.001456	-0.001656	-0.000740	0.000983	<CRD
A	0.18760	0.003045	-0.002198	-0.000600	0.000827	<CRD
B	0.18806	0.001217	-0.001846	-0.000658	0.000709	<CRD
C	0.13141	0.000821	-0.001132	-0.000478	0.000506	<CRD
D	0.13137	0.001666	-0.001333	-0.000472	0.000657	<CRD

rection of the strong axis (Y-axis) produced strains that closely matched and, in some cases, exceeded those obtained from the strain analysis in the direction of the weak axis (X-axis).

4 DISCUSSION

This study provides a comprehensive overview of the seismic performance of a wharf located in high seismic-risk regions. The investigation primarily focused on assessing the strain limits of the structure of this wharf, which was found to comply with the criteria outlined in ASCE 61-14. Following this, the influence of accidental torsion, accommodated by adjusting the offset value of lateral load eccentricity, was particularly significant for structures with an asymmetric center of mass position along the weak axis. In many designs of wharf for loading mining products, the presence of cranes and conveyors near the edge of the water resulted in an asymmetrical distribution of mass. Additionally, asymmetrical conditions were observed in the cross-section, where the freestanding length of the foundation piles increased as the wharf extended into the sea (hill-side building). These scenarios led to the prevalence of torsional behavior in the wharf structure. To analyze the seismic performance, nonlinear static analysis (pushover) was employed as a practical alternative to nonlinear time history analysis (NLTHA). However, it should be noted that once the new seismic map of Indonesia becomes available, it would be necessary to conduct a more comprehensive analysis with additional periods, including the 100-year return period (OLE: Operating Level Earthquake).

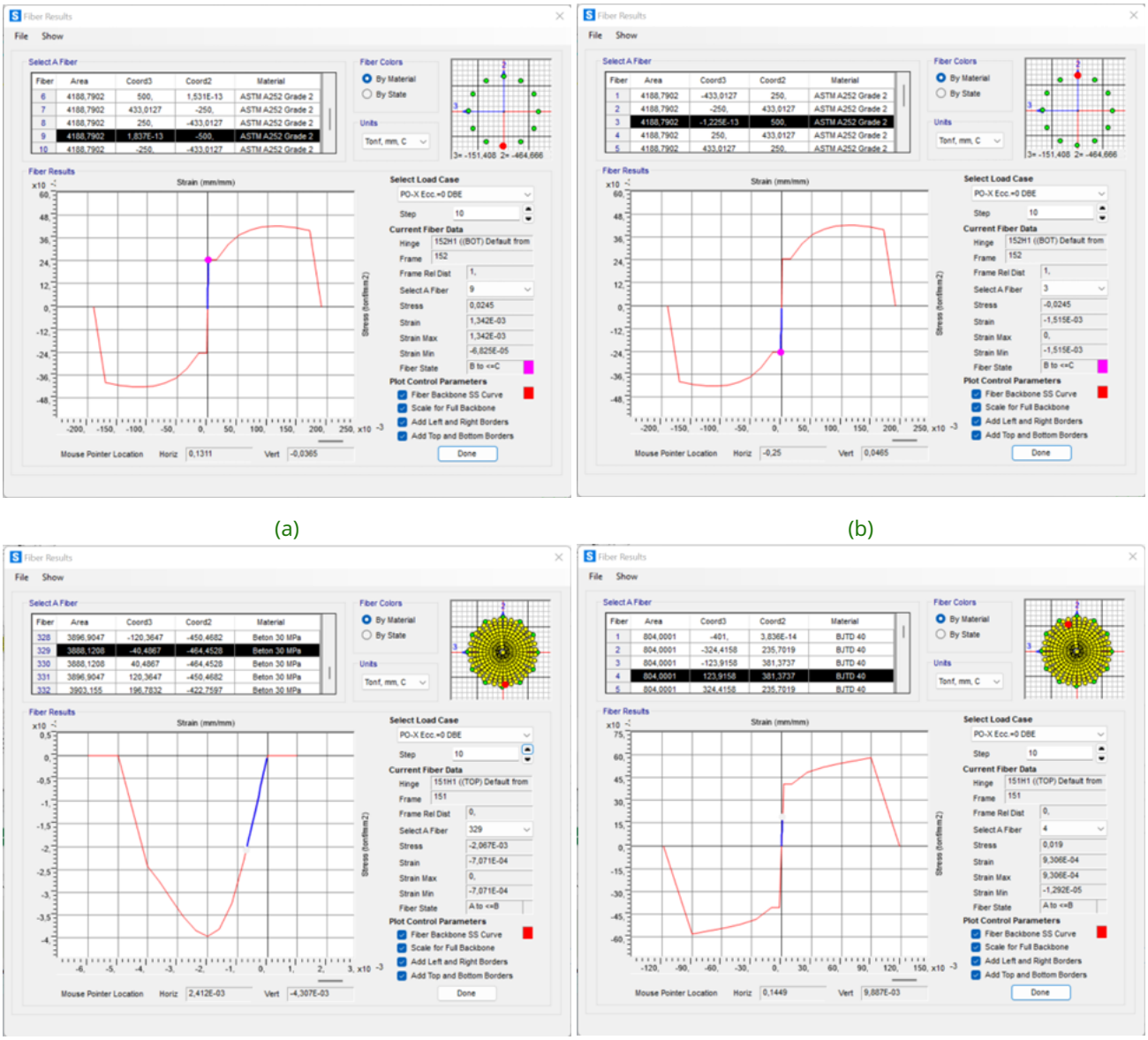

Figure 8 Strain on hinge component of $POX_{0\%}$-500_{yr}-X model (a) tension of steel pipe (b) compression of steel pipe (c) concrete (d) reinforcing steel.

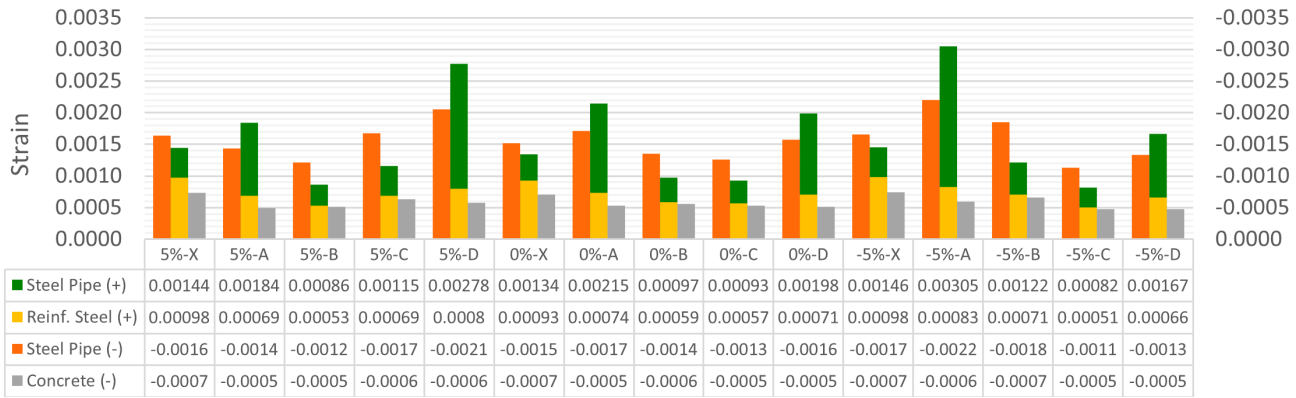

	5%-X	5%-A	5%-B	5%-C	5%-D	0%-X	0%-A	0%-B	0%-C	0%-D	-5%-X	-5%-A	-5%-B	-5%-C	-5%-D
Steel Pipe (+)	0.00144	0.00184	0.00086	0.00115	0.00278	0.00134	0.00215	0.00097	0.00093	0.00198	0.00146	0.00305	0.00122	0.00082	0.00167
Reinf. Steel (+)	0.00098	0.00069	0.00053	0.00069	0.0008	0.00093	0.00074	0.00059	0.00057	0.00071	0.00098	0.00083	0.00071	0.00051	0.00066
Steel Pipe (-)	-0.0016	-0.0014	-0.0012	-0.0017	-0.0021	-0.0015	-0.0017	-0.0014	-0.0013	-0.0016	-0.0017	-0.0022	-0.0018	-0.0011	-0.0013
Concrete (-)	-0.0007	-0.0005	-0.0005	-0.0006	-0.0006	-0.0007	-0.0005	-0.0006	-0.0005	-0.0005	-0.0007	-0.0006	-0.0007	-0.0005	-0.0005

Figure 9 Strain of hinge component for pushover in X-axis under the 500-year return period earthquake scenario

Table 3. Displacement, strain, and performance level for pushover in Y-axis under the 500-year return period earthquake

Node	Displacement (m)	Steel Pipe		Concrete	Reinf. Steel	Performance Level
		Strain (Tension)	Strain (Compression)	Strain (Compression)	Strain (Tension)	
Performance Point PO-Y Eccentricity = +0.05						
X	0.15877	0.00135	-0.001606	-0.000712	0.000951	<CRD
A	0.14338	0.001885	-0.001468	-0.000491	0.000677	<CRD
B	0.16404	0.001206	-0.001207	-0.000545	0.000786	<CRD
C	0.16329	0.001066	-0.001391	-0.000576	0.000667	<CRD
D	0.14389	0.001283	-0.002095	-0.000553	0.000490	<CRD
Performance Point PO-Y Eccentricity = 0.00						
X	0.15858	0.001348	-0.001603	-0.000712	0.000950	<CRD
A	0.14477	0.001898	-0.001491	-0.000493	0.000681	<CRD
B	0.16336	0.001202	-0.001199	-0.000539	0.000784	<CRD
C	0.16272	0.001059	-0.001385	-0.000571	0.000662	<CRD
D	0.14521	0.001304	-0.002105	-0.000553	0.000496	<CRD
Performance Point PO-Y Eccentricity = -0.05						
X	0.15836	0.001346	-0.001599	-0.000711	0.000949	<CRD
A	0.14614	0.001912	-0.001513	-0.000495	0.000684	<CRD
B	0.16266	0.001198	-0.001192	-0.000532	0.000781	<CRD
C	0.16211	0.001053	-0.001378	-0.000567	0.000658	<CRD
D	0.14650	0.001324	-0.002115	-0.000553	0.000502	<CRD

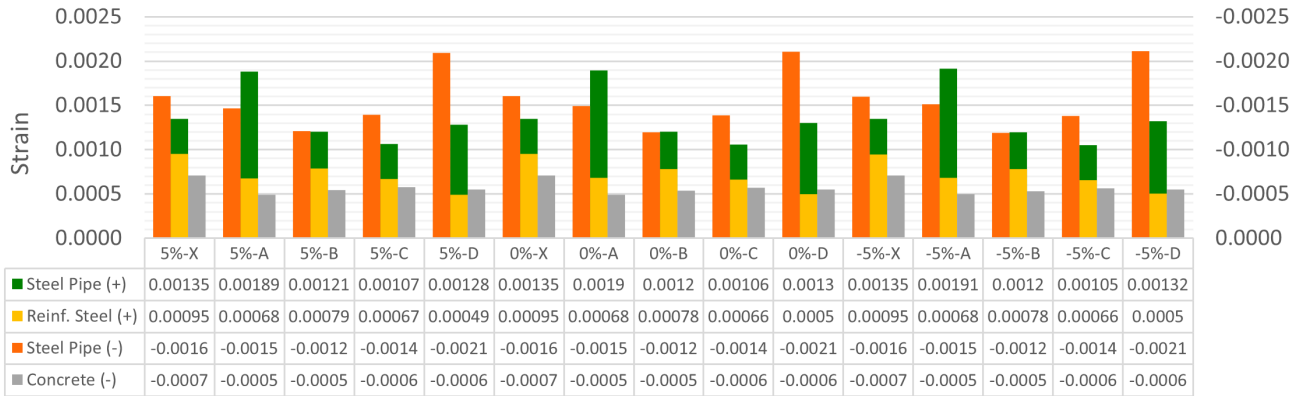

Figure 10 Strain of hinge component for pushover in Y-axis under the 500-year return period earthquake scenario

5 CONCLUSIONS

In conclusion, 30 models were analyzed in this study, and the obtained results showed that the structure continually experienced controllable and repairable damage following an earthquake scenario with a return period of 475 years. The structure exhibited inherent torsion, as evidenced by the variation in the obtained displacement control point values. Furthermore, it was found that the introduction of lateral load eccentricity offsets and the employment of varying pushover loading directions led to an increased displacement and strain experienced by the plastic hinge components. For further studies, it is imperative to conduct a more comprehensive investigation using NLTHA, taking into account the OLE hazard level and the constraints associated with the lower-to-upper bound values of the ground spring.

DISCLAIMER

The authors declare no conflict of interest.

ACKNOWLEDGMENTS

This study was supported by the Department of Civil and Environmental Engineering and LKFT Universitas Gadjah Mada, Yogyakarta, Indonesia.

REFERENCES

Applied Technology Council, ATC-40 (1996), *ATC 40: Seismic Evaluation and Retrofit of Concrete Buildings*, Seismic Safety Commission, California: ATC.

ASCE (2014), *ASCE 61-14: Seismic Design of Piers and Wharves*, ASCE, California.

ASCE 7 (2010), *Minimum Design Loads for Buildings and Other Structures*, 7th–10th edn, ASCE, Virginia.

ASCE 7 (2016), *Minimum Design Loads for Buildings and Other Structures*, 7th–16th edn, ASCE, Virginia.

ASCE 7 (2022), *Minimum Design Loads for Buildings and Other Structures*, 7th–22nd edn, ASCE, Virginia.

Bergman, A. W., Story, S. M., Howard, T. A. and Lighty, T. A. (2016), Seismic Design of an Irregular Wharf Utilizing ASCE 61, *in* 'Ports 2016', pp. 273–282.

Bruin, W., Goel, R. and Galbraith, J. (2016), Comparison of Procedures for Computing Seismic Displacement Demand for Concrete Piers and Wharf Structures, *in* 'Ports 2016', pp. 567–576.

FEMA (2011), 'FEMA P-55, Coastal construction manual: Principles and practices of planning, siting, designing, constructing, and maintaining residential buildings in coastal areas'.

FEMA, P. (2000), 'Commentary for the seismic rehabilitation of building, FEMA-356, Federal Emergency Management Agency', *Washington, DC* .

Goel, R. and Goel, H. (2017), Convergence behavior of substitute structure method in MOTEMS, *in* 'Proceedings of the 16th World Conference on Earthquake Engineering Paper', number 0350, pp. 9–13.

Goel, R. K. (2018), 'Evaluation of a substitute structure method to estimate seismic displacement demand in piers and wharves', *Earthquake Spectra* **34**(2), 759–772.

Hanifah, Y., Budipriyanto, A. and Rahardjo, I. (2017), Seismic Performance Evaluation of A Pile-supported pier in Aceh, Indonesia, *in* 'IOP Conference Series: Materials Science and Engineering', Vol. 267, IOP Publishing, p. 012022.

Nasional, B. S. (2019), 'SNI 1726:2019 Tata Cara Perencanaan Ketahanan Gempa untuk Struktur Bangunan Gedung dan Nongedung'.

Palma-ochoa, M. and Vasquez, L. (2019), Performance-based seismic assessment for pile-supported wharves – A case Study, *in* '12th Canadian Conference on Earthquake Engineering', pp. 1–8.

POLB (2012), 'Port of Long Beach Wharf Design Criteria Version 3.0', California.

POLB (2015), 'Port of Long Beach Wharf Design Criteria Version 4.0', California.

POLB (2021), 'Port of Long Beach Wharf Design Criteria Version 5.0', California.

Sandoval, J. D., Smith-Pardo, J. P. and Reyes, J. C. (2019), Evaluation of ASCE 61-14 Nonlinear Static Procedures for Estimating the Seismic Response of Wharves, *in* '15th Triennial International Conference', American Society of Civil Engineers Reston, VA, pp. 175–184.

Su, L., Wan, H., Lu, J., Ling, X., Elgamal, A. and Arulmoli, A. (2021), 'Seismic Performance Evaluation of A Pile-Supported Wharf System At Two Seismic Hazard Levels', *Ocean Engineering* **219**(November 2020), 108333.
URL: *https://doi.org/10.1016/j.oceaneng.2020.108333*

Terzaghi, K. (1955), 'Evaluation of coefficient of subgrade reaction, Geotechnique, Institution of Civ'.

The Overseas Coastal Area Development Institute of Japan, OCDI (2009), *Technical Standards and Commentaries for Port and Harbour Facilities in Japan*, The Overseas Coastal Area Development Institute of Japan, Tokyo.

Venkatalakshmi, P., Sree, J. and Rao, P. V. (2017), 'Performance Based Design of Jetties', *International Journal of Innovative Research in Science, Engineering and Technology* **6**(8).

Zacchei, E., Lyra, P. H. and Stucchi, F. R. (2019), 'Nonlinear static analysis of a pile-supported wharf', *Revista IBRACON de Estruturas e Materiais* **12**, 998–1009.